

Search for pulsating pre-main sequence stars in NGC 6383 ^{*}

K. Zwintz^{1†}, M. Marconi², P. Reegen¹, W.W. Weiss¹

¹*Department of Astronomy, University of Vienna, Türkenschanzstraße 17, A-1180 Vienna, Austria*

²*Osservatorio Astronomico di Capodimonte, Via Moiariello 16, 80131 Napoli, Italy*

Accepted . Received ; in original form

ABSTRACT

A search for pulsating pre-main sequence (PMS) stars was performed in the young open cluster NGC 6383 using CCD time series photometry in Johnson B & V filters. With an age of only ~ 1.7 million years all cluster members later than spectral type A0 have not reached the ZAMS yet, hence being ideal candidates for investigating PMS pulsation among A and F type stars. In total 286 stars have been analyzed using classical Fourier techniques. From about a dozen of stars within the boundaries of the classical instability strip, two stars were found to pulsate: NGC 6383 #170, with five frequencies simultaneously, and NGC 6383 #198, with a single frequency. In addition, NGC 6383 #152 is a suspected PMS variable star, but our data remain inconclusive. Linear, non-adiabatic models assuming PMS evolutionary phase and purely radial pulsation were calculated for the two new PMS pulsators. NGC 6383 #170 appears to pulsate radially in third and fifth overtones, while the other three frequencies seem to be of non-radial nature. NGC 6383 #198 pulsates monoperiodically, most probably in the third radial overtone.

Magnitudes and $B - V$ colours were available in the literature for only one third of all stars and we used them for calibrating the remaining.

Key words: techniques: photometric, stars: pre-main sequence, stars: variables: δ Scuti, galaxy: open clusters and associations: NGC 6383

1 INTRODUCTION

The study of the first stages in the formation of stars is one of the currently most active research fields in stellar astronomy. Pre-main sequence (PMS) stars lie between the birthline and the zero-age main sequence (ZAMS) in the Hertzsprung-Russell (HR) diagram. They are often characterized by a high degree of activity, strong near- or far-IR excesses and – in most cases – emission lines. They show photometric and spectroscopic variability on time scales of minutes to years, indicating that stellar activity begins in the earliest phases of stellar evolution. During the contraction towards the main sequence intermediate mass PMS stars possess temperatures and luminosities similar to evolved stars in the classical instability strip. This fact suggests that at least part of their activity is due to stellar pulsation.

The existence of pulsating PMS stars was first suggested by Breger (1972), who discovered in the young open cluster NGC 2264 δ Scuti-like pulsation in two PMS stars. Subsequent observations revealed similar oscillations in several Herbig Ae/Be field stars, e.g. HR 5999 (Kurtz & Marang

1995), as well as in PMS members of the young open cluster NGC 6823 (Pigulski, Kolackowski & Kopacki 2000). All known PMS pulsators populate the spectral range between A2 and F5, their periods lie between 18 minutes (Amado et al. 2004) and several hours, and their amplitudes are at millimagnitude level.

The evolutionary tracks for pre- and post main sequence stars intersect such that stars of fundamentally different evolutionary state have the same effective temperature and luminosity (Breger & Pamyatnykh 1998). Hence, the determination of the evolutionary state of a field star may be ambiguous. Therefore, young open clusters are most suitable to search for pulsating PMS stars.

2 THE YOUNG OPEN CLUSTER NGC 6383

The open cluster NGC 6383 ($\alpha_{2000} = 17^{\text{h}}34^{\text{m}}8$, $\delta_{2000} = -32^{\circ}34'$) is only ~ 1.7 Myr old and belongs to the Sgr OB1 association (together with NGC 6611, NGC 6530 and NGC 6531). It has a diameter of ~ 20 arcminutes and is centered around the bright spectroscopic binary HD 159176.

Eggen (1961) studied the stars in NGC 6383 using photoelectric photometry and found that all stars later than A0 lie above the ZAMS. Thé (1965) performed a photo-

^{*} based on observations with the 0.9m telescope at Cerro Tololo Interamerican Observatory (CTIO), La Serena, Chile.

[†] E-mail: zwintz@astro.univie.ac.at

graphic study in a circular area of ~ 12 arcminutes radius and could confirm Eggen's results. The core of the cluster was investigated by Fitzgerald et al. (1978) using photoelectric photometry to derive an average colour excess $E(B - V) = 0.33 \pm 0.02$, a cluster distance of 1.5 ± 0.2 kpc, an apparent distance modulus $V - M_V = 11.90 \pm 0.25$ corresponding to $(m - M)_0 = 10.9$ (adopted for our analysis) and a cluster age of 1.7 ± 0.4 Myr. The spectral energy distributions of stars in the central part of NGC 6383 were studied by Thé et al. (1985) with photoelectric photometry in the Walraven *WULBV*, Cousins *VRI* and Near-IR *JHKLM* photometric systems. Their derived colour excess $E(B - V) = 0.3 \pm 0.01$ and distance of 1.4 ± 0.15 kpc agree well with the values by Fitzgerald et al. (1978). Van den Ancker, Thé & de Winter (2000) investigated the central part of this cluster using low-resolution CCD spectroscopy and confirmed that all stars later than A0 lie above the ZAMS. They also report that several cluster members show an infrared excess, indicative of the presence of circumstellar dust, heated by the central star. They found H_α in emission only for their star #4 and identified it as a new Herbig Ae star.

All these characteristics make NGC 6383 an ideal target for the search of PMS pulsating stars.

3 OBSERVATIONS & DATA REDUCTION

CCD photometric time series in Johnson *B* & *V* filters were obtained with the 0.9m telescope at the Cerro Tololo Inter-american Observatory (CTIO), Chile, from Aug 11 to Aug 24, 2001, using the 2084 x 2046 SITe CCD chip, which provides a field of view (fov) of $\sim 13 \times 13$ arcminutes. In total, 53.25 hours photometry could be acquired within 8 clear nights.

The basic reductions (bias subtraction, flat-fielding) were performed using standard IRAF routines. The Multi Object Multi Frame (MOMF) software developed by Kjeldsen & Frandsen (1992) was used to extract the photometric signal. MOMF is optimized to analyze photometric time series (i.e. a large number of CCD frames per night) of semi-crowded fields by combining point-spread function fitting and aperture photometry. MOMF determines absolute and relative magnitudes of each star identified on the frames and their corresponding standard deviations. The absolute values are raw, uncorrected, instrumental magnitudes, whereas the relative light curves are determined by subtracting a weighted mean of all stars on the frame. Variable and non-variable, extremely red or blue stars are used to determine the weighted mean, requiring colour-dependent extinction corrections (see Sect. 3.1).

286 stars have been identified (see Fig.1) for which light curves using the optimum aperture producing minimal point-to-point scatter were generated. Nightly means were subtracted to correct for zero-point changes and long-term irregular light variations which probably are due to variable extinction by circumstellar dust.

For all 286 stars, a detailed frequency analysis was performed in both filters using the Fourier Analysis program Period98 (Sperl 1998) which is based on the Discrete Fourier Transformation (DFT, Deeming 1975) and provides a multi-sine fit option. A signal was considered to be significant if it

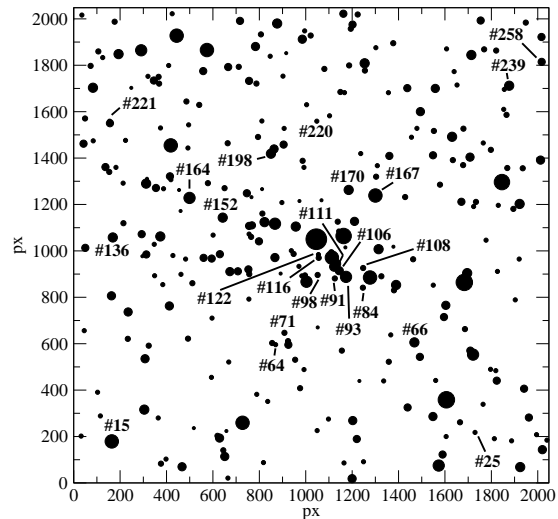


Figure 1. Schematic map of the observed field of NGC 6383 (fov $\sim 13 \times 13$ arcminutes, South is at the top and East is to the left) with all stars measured in Johnson *B* & *V* in pixels, where 1 px corresponds to 0.33 arcseconds. Identifiers refer to the objects discussed in the text.

exceeds four times the noise level in the amplitude spectrum. (Kuschnig et al. 1997).

Our own star numbers are used, cross references with the literature are given according to the publications by Fitzgerald et al. (1978), e.g. NGC 6383 #F4, by Thé (1965), e.g. NGC 6383 #T47, and Evans (1978), e.g. NGC 6383 #EV281.

3.1 Colour-dependent extinction

A systematic effect was encountered for differential light curves of some stars. Towards the end of the nights some stars became continuously brighter, but others fainter. The corresponding Bouguer plots (i.e. magnitude vs. airmass) showed that different colours were the explanation. Hence, the extinction correction had to include also the colour-dependent coefficient k' (Sterken & Manfroid 1992) in:

$$m = m_0 - (k^0 + k' \cdot CI) \cdot X, \quad (1)$$

where m_0 is the uncorrected magnitude, X is the airmass and k^0 the principal extinction coefficient. In our case, the colour index CI was taken as $(B - V)$.

The $(B - V)$ values available in the literature for 97 stars show a clear correlation with the slope, k , of the Bouguer plots (see Fig. 2). The relation between the 97 stars with $(B - V)$ from the literature and the instrumental $(B - V)$ values from our observations is modelled by an inverse second-order polynomial (solid line in Fig. 2). The three polynomial coefficients evaluate to $a_0 = -0.712 \pm 0.052$, $a_1 = +0.692 \pm 0.084$ and $a_2 = +0.177 \pm 0.029$. $(B - V)_{instr}$ values for all stars could then be transformed to the standard system according to:

$$(B - V)_{trans} = \sqrt{\frac{a_1^2}{4a_2^2} + \frac{((B - V)_{instr} - a_0)}{a_2}} - \frac{a_1}{2a_2} \quad (2)$$

where $(B - V)_{trans}$ are the transformed indices and $(B - V)_{instr}$ are our instrumental values (see Fig. 2).

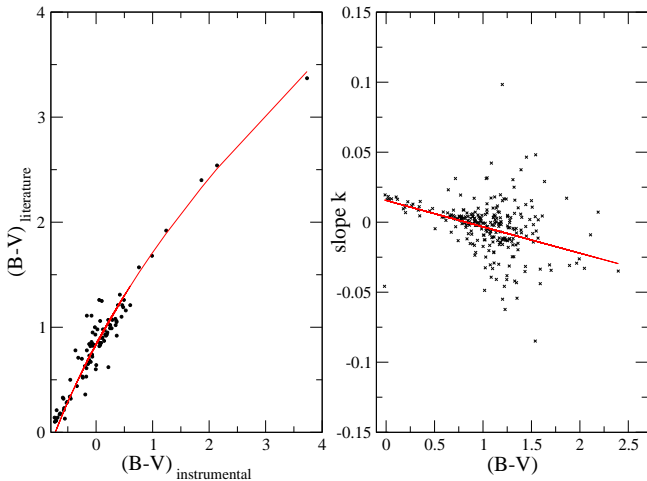


Figure 2. Modelling the colour-dependent extinction effect: *left:* Determination of the $(B - V)_{trans}$ of all stars using an inverse second-order polynomial (solid line) which describes the relation between instrumental and literature $(B - V)$ values for 97 of 286 stars. *right:* Dependence of the slope of the Bouguer plot, k , on $(B - V)_{trans}$ and weighted linear regression. As an example, data from the 8th night are shown in this figure, where the slope of the regression is 0.019 ± 0.010

4 VARIABLE STARS

About a dozen PMS cluster members have been selected as prime candidates to search for pulsation in NGC 6383 due to their spectral type and/or position in the HR-diagram. The major criterion has been the location of the stars in the region of the classical instability strip. But only two stars clearly show δ Scuti-like pulsation within our data, NGC 6383 #170 ($\alpha_{2000.0} = 17^{\text{h}}34^{\text{m}}37^{\text{s}}.8$, $\delta_{2000.0} = -32^{\circ}36'19''.5$) and NGC 6383 #198 ($\alpha_{2000.0} = 17^{\text{h}}34^{\text{m}}48^{\text{s}}.4$, $\delta_{2000.0} = -32^{\circ}37'21''.6$), and for NGC 6383 #152 pulsation can only be suspected.

The other PMS candidates for pulsation remain inconclusive in our data (e.g. they show variability only in one filter or the data quality is not good enough) and therefore need further investigation.

4.1 Pulsating PMS stars

4.1.1 NGC 6383 #170 (#F4)

For NGC 6383 #170 ($V = 12.61$ mag), Thé, Hageman & Westerlund (1985) found H_{α} in emission and a large amount of excess radiation in the NIR, typical for Herbig Ae/Be stars. With a spectral type of A5 IIIp, a confirmed membership to NGC 6383, and a position above the ZAMS #170 is a newly discovered PMS pulsator (see Fig. 3). Five frequencies spanning a period range between 1.24 and 2.89 hours have been detected. These frequencies, Johnson B & V amplitudes and phase shifts are listed in Table 1. All amplitude and phase errors were computed using the software package `epsim` (Reegen 2003).

Linear, non adiabatic pulsation was calculated for radial modes of PMS models resulting in three possible so-

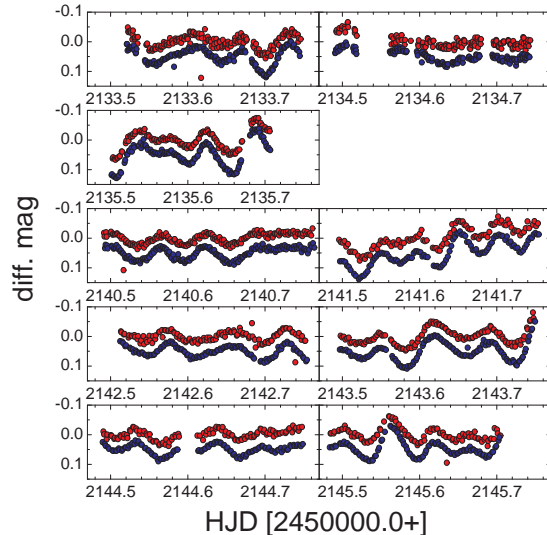


Figure 3. Differential light curves of the pulsating PMS star NGC 6383 #170: *top:* V filter, *bottom:* B filter (shifted for better visibility)

Table 1. Frequencies, amplitudes and (Δ phase) of phase(V) - phase(B) determined for the two PMS pulsators NGC 6383 #170 and NGC 6383 #198, as well as for NGC 6383 #15, which most probably is a foreground star; the errors in the last digits of the corresponding quantities are given in parentheses.

star	no	frequency [d ⁻¹]	V amp. [mmag]	B amp. [mmag]	Δ phase
#170	f1	14.376	12.5(8)	16.0(6)	-0.243(8)
	f2	19.436	11.3(3)	14.9(5)	-0.092(7)
	f3	13.766	9.8(4)	12.3(7)	0.474(8)
	f4	8.295	8.6(7)	11.1(7)	0.035(6)
	f5	17.653	7.6(9)	9.8(5)	-0.050(9)
#198	f1	19.024	20.8(9)	26.4(6)	0.114(3)
#15	f1	14.587	8.5(3)	8.4(3)	0.389(4)
	f2	16.972	4.0(3)	6.2(2)	-0.605(4)

lutions. No model reproduces all five frequencies simultaneously, but given the probable coexistence of radial and nonradial modes in these stars this could simply mean that not all frequencies correspond to radial pulsation. The model fitting the observed frequencies best, gives a stellar mass of $2.5M_{\odot}$, $\log L/L_{\odot} = 1.68$, $T_{\text{eff}} = 8100\text{K}$, and pulsation in third (f1) and fifth overtones (f2). The solution seems to be optimal, because it is closest to the parameters derived spectroscopically by van den Ancker, Thé & de Winter (2000): $\log L/L_{\odot} = 1.69$ and $T_{\text{eff}} = 8090\text{K}$ (filled symbol in Fig. 4).

4.1.2 NGC 6383 #198 (#T55)

Only one frequency of 19.024 d^{-1} , corresponding to a period of ~ 1.26 hours, is significant in both filters (see Table 1), but the light curve shown in Fig. 5 indicates multi-periodicity.

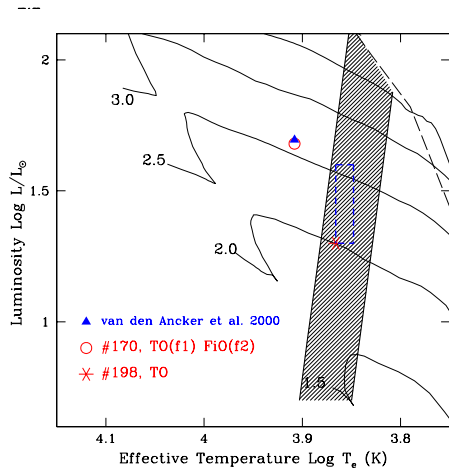


Figure 4. Linear, non-adiabatic radial pulsation models for NGC 6383 #170 and #198: solid lines are PMS evolutionary tracks for 1.5, 2.0, 2.5 and 3.0 M_{\odot} (Palla & Stahler, 1993); the open circle denotes the model for #170 reproducing the observed frequencies best (see text for detailed explanation), the filled triangle marks the position of the observed values for #170 derived by van den Ancker, Thé and de Winter (2000); the star shows the optimum model for #198; the dashed box indicates the empirical ranges of $\log T_{\text{eff}}$ and $\log L/L_{\odot}$ for #198; the shaded area is the theoretical PMS instability strip for the first three radial modes (Marconi & Palla, 1998).

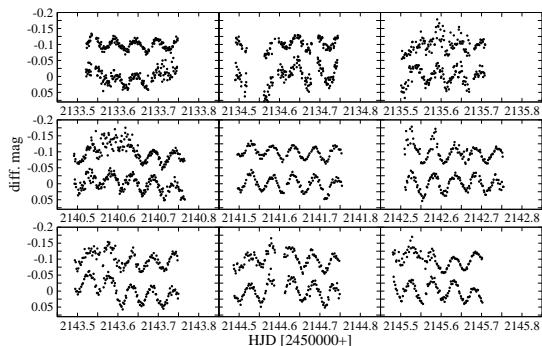


Figure 5. Differential light curves of the PMS pulsator NGC 6383 #198: *top*: V filter (shifted for better visibility), *bottom*: B filter

Calculations of linear, non-adiabatic, radial pulsation models were performed (see Fig. 4). As no spectral classification is available for this star, the V and $(B - V)$ values were used to derive empirical ranges of luminosity and effective temperature based on the transformations given by Kenyon & Hartmann (1995). These ranges are indicated by the dashed box in Fig. 4. Only for pulsation in the third overtone (TO) the theoretical models have temperatures and luminosities close to the observations. Such a high overtone mode is rather difficult to explain in case of monop periodic pulsation, other modes may be buried in the noise.

Relying on the cluster membership of NGC 6383 #198, it seems reasonable that the star pulsates with a single frequency in the third radial overtone having $2.0M_{\odot}$, $\log L/L_{\odot} = 1.3$ and $T_{\text{eff}} = 7345K$.

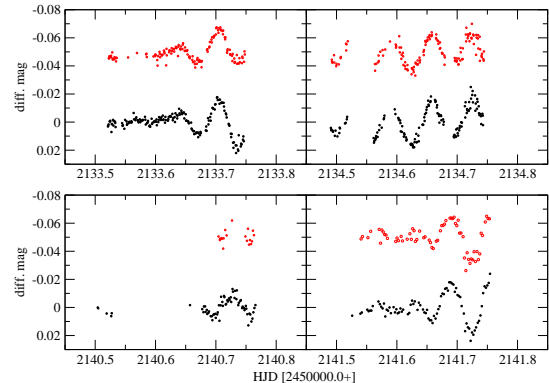


Figure 6. Differential, relative light curves of NGC 6383 #15: *top*: V filter (shifted for better visibility), *bottom*: B filter

4.1.3 NGC 6383 #152 (#T54)

With $(B - V) = 0.57$ mag #152 falls within the boundaries of the classical instability strip (Fig. 10). But only one significant frequency of 2.55 d^{-1} with a peak-to-peak amplitude of ~ 30 mmag appears in the B data. Unfortunately the V filter data are of worse quality, where the noise is so dominant that no peak in the amplitude spectrum exceeds four times the noise level.

Although this star has been one of the primary targets in NGC 6383 to search for PMS pulsators, it remains inconclusive in our data. Longer time series of better quality have to be obtained to unambiguously decide about variability.

4.2 Other Variables

For several other stars, that probably are not pulsating PMS cluster members, variability could also be detected. A list of suspected variable stars is given in Table 2.

4.2.1 NGC 6383 #15 (#T47)

$V = 10.03$ mag and $(B - V) = 0.34$ mag together with its position in the HR-diagram indicate that this star is not a member of the cluster. Two frequencies, corresponding to periods of 1.645 and 1.414 hours, were found to be significant (see Table 1). As it is most likely in the foreground, it seems to be a classical δ Scuti type star (see Fig. 6). The amplitude and phase errors were computed using the software package *epsim* (Reegen 2003).

4.2.2 NGC 6383 #25

No astrophysical parameters were available from the literature for NGC 6383 #25. Our transformation yields $V = 16.77$ mag and $B - V = 1.58$ mag. A frequency of 1.19755 d^{-1} , i.e. a period of 20.04 hours, leads to a phase plot shown in Fig. 7.

$(B - V) = 1.58$ mag corresponds to a spectral type of M5 and is associated to $M/M_{\odot} = 0.21$, and $R/R_{\odot} = 0.27$ according to Schmidt-Kaler (1965). Assuming a rotation period of 20.04 hours, the equatorial rotational velocity is

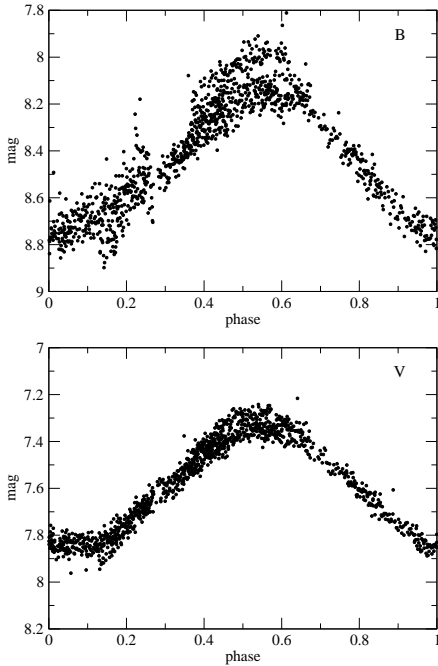


Figure 7. Phase plot of NGC 6383 #25: *top*: B filter, *bottom*: V filter

16.37 km s^{-1} . This velocity would be in agreement with a rotating, active and weak-lined T Tauri star.

4.2.3 NGC 6383 #71

No astrophysical information was available from the literature for NGC 6383 #71. Our calculations give $V = 15.37$ mag and $(B - V) = 1.35$ mag. If the star belongs to the cluster, it is an early K type star (Schmidt-Kaler 1965).

Two frequencies of 2.759 and 2.240 d^{-1} , i.e. periods of 8.688 and 10.714 hours, respectively, were detected (Fig. 8). A variability on this time scale cannot be explained assuming cluster membership. Permitting NGC 6383 #71 to be more distant than the cluster itself, interstellar reddening may shift its position in the HR-diagram into the SPB, or β Cephei domain. A clear decision can only be drawn from spectroscopy.

4.2.4 NGC 6383 #64

No information about this star was found in the literature. According to our observations, the star has only 16.72 mag in V and $(B - V) = 1.63$ mag. A single frequency of $\sim 2.499 \text{ d}^{-1}$ (corresponding to a period of 9.605 hours) with a peak-to-peak amplitude of approximately 20 mmag is found to be significant in both B and V light curves and leads to the phase plot shown in Fig. 9.

5 CONCLUSIONS

Photometric time series of 286 stars in the field of the young open cluster NGC 6383 were analyzed using classical Fourier

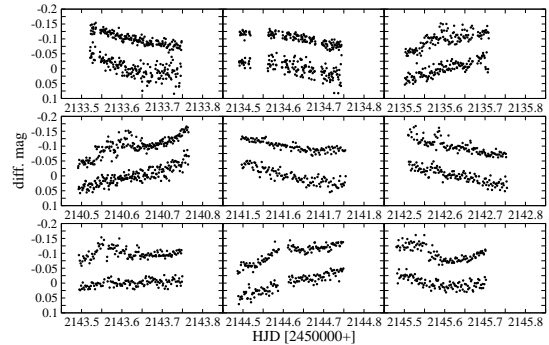


Figure 8. Differential light curves of NGC 6383 #71: *top*: V filter (shifted for better visibility), *bottom*: B filter

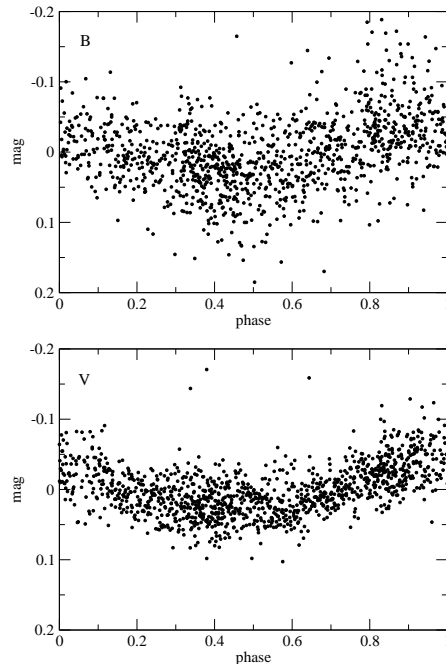


Figure 9. Phase plot of NGC 6383 #64: *top*: B filter, *bottom*: V filter

techniques in order to detect pulsation among PMS members of spectral types A to F. A higher number of PMS pulsators would allow to confine the boundaries of the PMS instability strip observationally and especially investigate a possible difference to the classical instability region.

The computed V and $(B - V)$ values were dereddened using $E(B - V) = 0.33 \pm 0.02$ mag and the apparent distance modulus of $V - M_V = 11.90 \pm 0.25$ corresponding to $(m - M)_0 = 10.9$ and a distance of 1.5 ± 0.2 kpc derived by Fitzgerald et al. (1978). Out of 15 cluster members that fall in the region of the classical instability strip (see Fig. 10), for only two, NGC 6383 #170 and NGC 6383 #198, pulsation could be clearly detected, whereas for NGC 6383 #152 variability can only be suspected. This corresponds to $\lesssim 20\%$ variable stars within the region of the classical instability

Table 2. Variables and suspected variables in the field of NGC 6383: *star* denotes our star number and *ref* the cross reference with the literature (according to F ... Fitzgerald et al. (1978), T ... Thé (1965)), M_v and $(B - V)_0$ are derived using $E(B - V) = 0.33$ mag and $V - M_v = 11.9$ mag, the spectral types (*sp*) are taken from the literature

star #	ref	V mag	B-V mag	M_v mag	$(B - V)_0$ mag	sp	var. in filter B / V / B & V	remarks
170	F 4	12.61	0.60	1.00	0.37	A5	B & V	new PMS pulsator
198	T 55	12.90	0.36	0.93	0.3	-	B & V	new PMS pulsator
152	T 54	12.45	0.70	0.44	0.24	-	B & V	suspected PMS pulsator
15	T 47	10.08	0.34	-1.87	0.01	-	B & V	foreground δ Scuti star
25	-	16.77	1.58	4.87	1.25	-	B & V	T Tauri star
64	-	16.72	1.63	4.82	1.30	-	B & V	probably not a cluster member
71	-	15.37	1.35	3.47	1.02	-	B & V	probably not a cluster member
66	T 28	12.59	0.33	0.63	-0.17	-	B	inconclusive in V
84	-	15.98	1.31	4.08	0.99	-	B	inconclusive in V
91	F 10	15.3	0.9	3.41	0.62	-	B	inconclusive in V
93	F 20	11.42	0.17	-0.43	-0.24	B8	B & V	different periods in B & V
98	F 11	15.10	1.06	3.26	0.81	-	B & V	T Tauri candidate
106	F 6	13.77	0.52	1.93	0.27	A6	B & V	known IR excess
108	-	15.61	1.45	3.71	1.12	-	B & V	P \sim 7.26 hours, inconclusive
111	F 8	12.82	0.32	1.00	0.00	-	B & V	P \sim 5.65 hours, inconclusive
116	-	15.13	1.31	3.23	0.98	-	B & V	T Tauri candidate
122	-	16.44	1.42	4.54	1.09	-	B & V	unresolvable
136	T 52	12.33	0.72	0.43	0.39	-	B	inconclusive in V
164	T 5	11.31	0.011	-0.6	-0.32	-	B & V	P \sim 2 days, amplitude \sim 30 mmag
167	F 3	10.3	0.29	-1.57	-0.05	-	B	saturated in V
220	-	16.67	2.03	4.77	1.70	-	V	P \sim 2.87 hours in V
221	-	16.54	1.19	4.64	0.86	-	B & V	irregular variable, T Tauri candidate
239	T 77	12.50	0.85	0.61	0.59	-	B & V	probably not a cluster member
258	-	14.56	0.69	2.66	0.69	-	B & V	different periods in B & V

strip in NGC 6383 down to a noise level of 0.2 mmag in V and 0.1 mmag in B in the Fourier domain. The percentage of detected pulsating PMS stars in the instability region is somewhat lower than is observed for their post-ZAMS counterparts.

A literature search was performed for additional information about all stars in NGC 6383. For the Herbig Ae star NGC 6383 #170, one of the two discovered pulsating PMS stars, van den Ancker, Thé & de Winter (2000) found a large infrared excess, H_α in emission, and indications for the presence of circumstellar gas in the spectrum. We support the idea of circumstellar material around NGC 6383 #170, because the raw photometric time series show additional irregular light variations on longer time scales than for pulsation. Only magnitude and colours are available in the literature for NGC 6383 #198, but its light curve and position in the HR-diagram provide clear evidence for another new PMS pulsator.

For all stars on the frames, V magnitudes and $B - V$ colours are given in Table A1 in the Appendix.

The location of 15 known PMS pulsators in the HR-diagram is shown in Fig. 11. The values for T_{eff} and L/L_\odot for the PMS pulsators are taken from Marconi & Palla (2003), Marconi (2004, priv. comm.), Amado et al. (2004) and Koen et al. (2003), the PMS evolutionary tracks from D’Antona & Mazzitelli (1994), the borders of the classical instability strip from Breger & Pamyatnykh (1998), where RE_{obs} marks the empirical red edge, BE the general blue edge for the radial overtones, and BE_F the blue edge for the fundamental mode. However, the number of known PMS

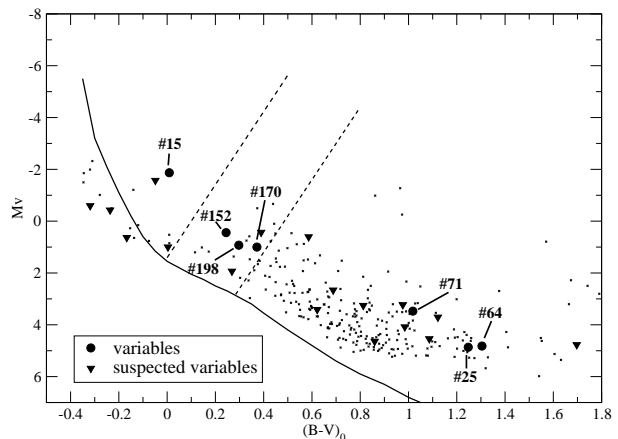


Figure 10. HR-diagram of NGC 6383, the Schmidt-Kaler ZAMS (solid line) and approximate location of the classical instability strip (dashed lines, adopted from Pamyatnykh 2000); small symbols: all analyzed stars, circles: variable stars, triangles: suspected variable stars.

pulsators remains insufficient to determine empirically the PMS instability strip.

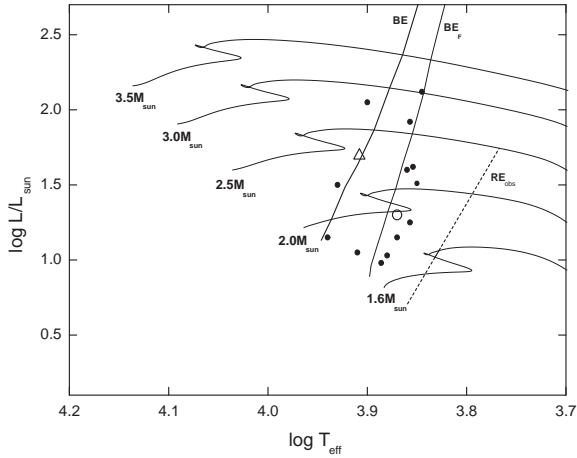


Figure 11. HR-diagram of 15 known PMS pulsators. The open triangle marks the position of NGC 6383 #170, the open circle the location of NGC 6383 #198. Also indicated are the PMS evolutionary tracks (D’Antona & Mazzitelli 1994), the empirical red edge (RE_{obs}), the theoretical blue edge for the fundamental mode (BE_F) and the general theoretical blue edge for the radial overtones (BE) of the classical instability strip. (Breger & Pamyatnykh 1998)

ACKNOWLEDGMENTS

This project was supported by the Austrian *Fonds zur Förderung der wissenschaftlichen Forschung* (P14984). Fourier Analysis was performed using the program PERIOD98 written by M. Sperl (1998). Use was made of the WEBDA database, operated at the Institute of Astronomy of the University of Lausanne. Finally, it is a pleasure to acknowledge E. Paunzen for valuable comments on data reduction, A. Pamyatnykh for fruitful discussions, as well as S. Frandsen and T. Arentoft for their patient introduction to the MOMF software.

REFERENCES

- Amado P.J., Moya A., Suárez J.C., Martín-Ruiz S., Garrido R., Rodríguez E., Catala C., Goupil M.J., 2004, MNRAS, preprint (astro-ph/6110A)
 Breger M., 1972, ApJ, 171, 539
 Breger M., Pamyatnykh A., 1998, A&A, 332, 958
 D’Antona F., Mazzitelli I., 1994, ApJS, 90, 467
 Deeming T.J., 1975, Ap&SS, 36, 137
 Eggen O.J., 1961, Roy. Obs. Bull., 27, 61
 Evans, T.L., 1978, MNRAS, 184, 661
 Fitzgerald M.P., Jackson P.D., Luiken M., Grayzeck E.J., Moffat A.F.J., 1978, MNRAS, 182, 607
 Kenyon S.J., Hartmann L., 1995, ApJS, 101, 117
 Kjeldsen H., Frandsen S., 1992, PASP, 104, 413
 Koen C., Balona L.A., Khadaroo K., Lane I., Prinsloo A., Smith B., Laney C.D., 2003, MNRAS, 344, 1250
 Kurtz D., Marang F., 1995, MNRAS, 276, 191

- Kuschnig R., Weiss W.W., Bahr R., Bely P., Jenkner H., 1997, A&A, 328, 544
 Marconi M., Palla F., 1998, AJ, 507, L141
 Marconi M., Palla F., 2003, Ap&SS, 284, 245
 Palla F., Stahler S.W., 1993, ApJ, 418, 414
 Pamyatnykh A., 2000, in Breger M., Montgomery M. H., eds., ASP Conf. Ser. 210, Delta Scuti and related stars. Astron. Soc. Pac., San Francisco, p. 215
 Pigulski A., Kolackowski Z., Kopacki G., 2000, in Szabados L., Kurtz D.W., eds., Proc. IAU Coll. 176, ASP Conf. Ser. 203, The impact of large scale surveys on pulsating star research. Astron. Soc. Pac., San Francisco, p. 499
 Reegen P., 2003, in Proc. of the Second EDDINGTON Workshop, Stellar Structure and Habitable Planet Finding, in press
 Schmidt-Kaler, Th., 1965 in Landolt-Börnstein, Numerical data and functional relationships in science and technology, group VI, vol. I, pp.284. Springer Verlag, Berlin
 Sperl M., 1998, Comm. Ast. 112, 1
 Sterken C., Manfroid J., 1992, Astronomical Photometry. Kluwer Academic Publishers
 Thé P.S., 1965, Contr. from the Bosscha Obs., No. 32
 Thé P.S., Hageman T., Westerlund B.E., Tjin A Djie H.R.E., 1985, A&A, 151, 391
 Van den Ancker M.E., Thé P.S., de Winter D., 2000, A&A, 362, 580

APPENDIX A: PHOTOMETRIC DATA

For all stars located on the CCD chip, V and $B - V$ values were computed using our transformation (described in Sect. 3.1). Assuming cluster membership they were dereddened using $E(B - V) = 0.33$ mag and $V - M_V = 11.9$ mag (Fitzgerald et al. 1978). The resulting photometric data (V , $B - V$, M_V and $(B - V)_0$) are listed in Table A1.

Table A1. Photometric data for all observed stars; cluster membership is assumed; *no* lists the star number, *ref* denotes the cross reference and star number in the literature, X and Y are coordinates in pixels on the CCD, M_V and $(B - V)_0$ were derived using $E(B - V) = 0.33$ mag and $V - M_V = 11.9$ mag (Fitzgerald et al. 1978).

no #	ref	X [px]	Y [px]	V [mag]	$(B - V)$ [mag]	M_V [mag]	$(B - V)_0$ [mag]
1	T 32	1199.72	18.23	13.431	0.713	1.531	0.383
2	-	664.68	20.66	16.263	1.290	4.363	0.960
3	T 13	1924.37	68.24	12.056	0.210	0.156	-0.120
4	T 38	466.83	69.62	13.627	0.758	1.727	0.428
5	T 19	1573.26	74.82	11.645	1.303	-0.255	0.973
6	-	375.99	82.95	15.563	0.878	3.663	0.548
7	-	1164.79	86.15	16.818	1.327	4.918	0.997
8	-	817.81	87.60	16.852	1.209	4.952	0.879
9	-	1248.96	91.15	16.866	1.144	4.966	0.814
10	-	397.82	102.68	16.438	1.060	4.538	0.730
11	T 39	651.10	114.00	13.374	0.672	1.474	0.342
12	EV 281	1589.78	122.32	14.596	1.706	2.696	1.376
13	-	644.77	140.70	15.357	1.046	3.457	0.716
14	T 12	2019.93	143.29	13.038	0.792	1.138	0.462
15	T 47	164.02	178.78	10.030	0.339	-1.870	0.009
16	-	1887.08	181.27	17.003	1.250	5.103	0.920
17	-	2039.42	184.29	16.689	1.225	4.789	0.895
18	T 31	1220.05	189.32	14.006	0.736	2.106	0.406
19	-	1812.81	190.70	16.166	1.133	4.266	0.803
20	T 40	628.59	193.29	13.264	0.605	1.364	0.275
21	-	1605.13	199.85	16.077	1.518	4.177	1.188
22	-	31.87	201.90	16.383	0.993	4.483	0.663
23	-	619.57	202.99	15.158	1.178	3.258	0.848
24	-	1994.76	208.01	16.794	1.219	4.894	0.889
25	-	1729.50	217.61	16.767	1.578	4.867	1.248
26	-	658.03	223.70	17.094	1.273	5.194	0.943
27	-	1049.01	225.60	16.861	1.186	4.961	0.856
28	-	517.64	236.29	17.093	2.194	5.193	1.864
29	T 41	727.62	259.08	10.913	1.192	-0.987	0.862
30	-	1664.79	261.29	15.050	0.843	3.150	0.513
31	T 30	1202.61	268.73	13.379	0.914	1.479	0.584
32	-	1097.97	275.27	16.731	1.346	4.831	1.016
33	-	364.16	280.00	16.741	1.164	4.841	0.834
34	-	1961.79	281.93	14.550	1.162	2.650	0.832
35	T 29	1548.39	286.17	13.655	0.818	1.755	0.488
36	-	115.06	288.75	16.779	1.049	4.879	0.719
37	T 46	304.32	316.07	12.675	0.759	0.775	0.429
38	-	1439.01	325.23	14.780	0.778	2.880	0.448
39	-	1764.32	338.96	16.081	1.105	4.181	0.775
40	-	836.25	351.06	16.542	1.428	4.642	1.098
42	-	788.92	381.86	16.293	1.240	4.393	0.910
43	-	102.83	390.66	16.382	1.196	4.482	0.866
44	-	1941.02	405.92	14.340	0.825	2.440	0.495
45	-	975.65	408.16	15.494	1.073	3.594	0.743
46	-	1231.15	439.34	17.018	1.304	5.118	0.974
47	EV 109	1335.71	439.39	16.672	1.114	4.772	0.784
48	-	1823.24	440.78	14.399	0.857	2.499	0.527
49	-	1559.90	441.50	16.519	1.588	4.619	1.258
50	-	593.61	454.80	16.441	1.152	4.541	0.822
51	-	1819.27	483.77	16.148	1.062	4.248	0.732
52	-	992.62	488.38	16.745	1.425	4.845	1.095
53	-	1796.40	489.68	16.211	1.112	4.311	0.782
54	-	668.14	520.89	16.908	1.558	5.008	1.228
55	EV 108	1357.83	522.08	15.690	1.204	3.790	0.874
56	-	954.27	530.73	15.653	1.136	3.753	0.806
57	T 45	307.36	535.32	13.276	2.410	1.376	2.080

cross references according to: T ... Thé (1965), EV ... Evans (1978),
F ... Fitzgerald et al. (1978)

Table A1 – continued Photometric data

no #	ref	X [px]	Y [px]	V [mag]	(B – V) [mag]	M_V [mag]	(B – V) ₀ [mag]
58	EV 107	1492.03	543.14	14.841	1.002	2.941	0.672
59	T 96	1721.10	553.00	11.403	0.704	-0.497	0.374
60	EV 111	1155.64	570.06	15.681	0.915	3.781	0.585
61	-	1709.27	570.10	14.552	0.920	2.652	0.590
62	EV 113	323.40	591.39	15.427	1.248	3.527	0.918
63	EV 380	925.06	595.27	14.190	0.667	2.290	0.337
64	-	870.31	595.94	16.721	1.634	4.821	1.304
65	-	855.11	602.99	15.481	1.335	3.581	1.005
66	T 28	1468.18	605.70	12.532	0.163	0.632	-0.167
67	-	923.89	611.24	15.374	1.115	3.474	0.785
68	-	233.11	621.07	15.116	0.982	3.216	0.652
69	EV 114	492.68	621.79	15.942	1.034	4.042	0.704
70	EV 110	1366.40	637.78	16.758	1.186	4.858	0.856
71	-	908.28	646.88	15.373	1.348	3.473	1.018
72	-	45.21	656.10	16.907	1.204	5.007	0.874
73	-	1686.12	662.89	15.174	0.926	3.274	0.596
74	EV 112	1051.58	670.23	17.131	1.262	5.231	0.932
75	EV 115	595.97	710.18	16.084	1.091	4.184	0.761
76	-	1595.67	714.97	14.665	0.891	2.765	0.561
77	T 44	234.60	736.71	13.560	0.706	1.660	0.376
78	T 43	412.39	762.81	13.103	0.445	1.203	0.115
79	EV 158	1603.79	765.28	13.797	0.691	1.897	0.361
80	-	1903.06	788.90	16.290	1.571	4.390	1.241
81	-	755.16	792.04	16.050	1.335	4.150	1.005
82	T 50	162.81	806.29	13.527	0.943	1.627	0.613
83	-	1380.35	830.01	15.077	1.358	3.177	1.028
84	-	1246.26	841.33	15.982	1.315	4.082	0.985
85	-	1549.76	852.24	16.491	1.283	4.591	0.953
86	T 17	1389.39	853.14	12.649	0.659	0.749	0.329
87	-	383.82	854.74	16.256	1.213	4.356	0.883
88	-	511.36	860.75	15.543	1.114	3.643	0.784
90	F 21	1003.22	867.06	12.000	0.773	0.100	0.443
91	F 10	1125.23	881.18	15.312	0.952	3.412	0.622
92	F 2	1277.07	885.23	10.403	-0.017	-1.497	-0.347
93	F 20	1173.62	888.08	11.473	0.094	-0.427	-0.236
94	-	1325.99	890.34	15.870	1.013	3.970	0.683
95	-	983.26	892.09	16.770	1.742	4.870	1.412
96	-	348.81	893.05	16.332	1.133	4.432	0.803
97	-	996.66	894.20	15.576	0.955	3.676	0.625
98	F 11	1051.19	896.15	15.155	1.143	3.255	0.813
99	-	462.23	898.94	16.814	1.409	4.914	1.079
100	-	756.70	899.89	15.735	1.348	3.835	1.018
101	-	891.73	902.12	17.578	1.650	5.678	1.320
102	T 7	1695.73	904.24	12.752	0.339	0.852	0.009
103	T 42	673.15	910.60	13.660	0.798	1.760	0.468
104	-	1826.27	911.37	16.469	1.250	4.569	0.920
105	-	707.38	911.91	14.043	1.142	2.143	0.812
106	F 6	1144.36	914.89	13.833	0.598	1.933	0.268
107	-	752.96	920.26	14.324	0.852	2.424	0.522
108	-	1247.24	926.33	15.608	1.452	3.708	1.122
109	F 7	1122.63	931.87	12.662	0.255	0.762	-0.075
110	-	970.63	933.44	16.568	1.441	4.668	1.111
111	F 8	1130.81	944.62	12.900	0.333	1.000	0.003
112	-	1462.80	963.98	15.573	1.100	3.673	0.770
113	-	482.24	964.66	16.406	1.044	4.506	0.714
114	EV 132	1920.00	964.68	16.575	2.313	4.675	1.983
115	-	594.66	967.04	14.272	0.987	2.372	0.657
116	-	1055.88	969.96	15.128	1.306	3.228	0.976

cross references according to: T ... Thé (1965), EV ... Evans (1978),
F ... Fitzgerald et al. (1978)

Table A1 – *continued* Photometric data

no #	ref	X [px]	Y [px]	V [mag]	(B – V) [mag]	M_V [mag]	(B – V) ₀ [mag]
117	-	559.77	970.03	14.200	0.848	2.300	0.518
118	F 9	1112.65	971.08	10.885	0.051	-1.015	-0.279
119	F 23	867.23	971.34	13.824	1.039	1.924	0.709
120	-	295.87	977.09	17.157	1.659	5.257	1.329
121	-	427.70	980.10	16.458	1.318	4.558	0.988
122	-	1054.97	984.20	16.442	1.416	4.542	1.086
123	-	313.07	984.63	14.516	1.048	2.616	0.718
124	EV 101	629.94	985.65	14.616	0.993	2.716	0.663
125	-	947.79	986.76	15.805	1.239	3.905	0.909
126	-	1110.64	994.16	15.072	1.298	3.172	0.968
127	-	938.11	1000.83	16.425	1.493	4.525	1.163
128	F 5	1313.96	1007.28	12.915	0.474	1.015	0.144
129	-	49.92	1013.16	14.420	1.379	2.520	1.049
130	-	1170.83	1015.02	17.255	1.962	5.355	1.632
131	-	1377.98	1018.00	17.168	1.582	5.268	1.252
132	-	347.13	1028.38	16.958	1.574	5.058	1.244
133	EV 118	798.36	1041.11	15.004	0.921	3.104	0.591
134	-	1777.01	1046.14	16.344	1.157	4.444	0.827
136	T 52	168.39	1057.81	12.333	0.719	0.433	0.389
137	-	764.65	1060.37	15.063	1.368	3.163	1.038
138	T 53	373.26	1062.19	12.364	0.845	0.464	0.515
139	F 14	1163.20	1064.25	9.908	0.011	-1.992	-0.319
140	EV 117	600.77	1068.02	16.079	3.436	4.179	3.106
141	EV 341	292.97	1072.18	14.870	0.673	2.970	0.343
142	-	755.79	1072.22	16.298	1.206	4.398	0.876
143	-	1142.33	1085.32	16.181	1.561	4.281	1.231
144	F 25	957.10	1104.88	12.546	0.193	0.646	-0.137
145	-	755.94	1107.58	14.528	0.920	2.628	0.590
146	-	768.08	1109.97	14.881	1.161	2.981	0.831
147	F 24	867.63	1117.11	11.401	0.099	-0.499	-0.231
148	-	214.36	1119.42	15.477	1.107	3.577	0.777
149	F 22	822.58	1123.93	12.344	0.586	0.444	0.256
150	-	1137.82	1125.75	15.797	1.118	3.897	0.788
151	F 18	1210.31	1127.16	13.414	0.895	1.514	0.565
152	T 54	642.20	1143.42	12.343	0.574	0.443	0.244
153	153	813.09	1160.87	15.900	1.043	4.000	0.713
154	EV 131	460.58	1172.03	17.089	1.410	5.189	1.080
155	-	1894.82	1181.04	15.942	1.326	4.042	0.996
156	-	1723.72	1191.24	16.841	1.260	4.941	0.930
157	-	1829.80	1196.28	16.631	1.169	4.731	0.839
158	T 84	1921.94	1202.35	12.173	0.177	0.273	-0.153
159	-	897.28	1208.26	16.722	1.459	4.822	1.129
160	-	1733.69	1211.13	15.075	1.104	3.175	0.774
161	-	1671.01	1211.58	14.758	0.802	2.858	0.472
162	-	972.84	1214.98	17.186	1.603	5.286	1.273
163	-	1067.84	1218.17	17.137	1.521	5.237	1.191
164	T 5	499.27	1228.13	11.307	0.011	-0.593	-0.319
165	-	766.29	1231.46	17.090	1.361	5.190	1.031
166	EV 105	1428.35	1232.13	15.391	1.282	3.491	0.952
167	F 3	1300.22	1238.68	10.329	0.281	-1.571	-0.049
168	EV 119	746.33	1248.59	14.920	0.952	3.020	0.622
169	-	454.11	1262.42	17.140	2.916	5.240	2.586
170	F 4	1185.09	1262.77	12.900	0.702	1.000	0.372
171	-	811.75	1266.25	17.083	1.403	5.183	1.073
172	-	387.18	1267.98	16.583	1.102	4.683	0.772
173	EV 120	650.21	1270.25	15.923	1.085	4.023	0.755
174	-	354.41	1271.08	14.232	1.321	2.332	0.991
175	EV 106	1578.70	1285.38	15.113	0.979	3.213	0.649

cross references according to: T ... Thé (1965), EV ... Evans (1978),
F ... Fitzgerald et al. (1978)

Table A1 – continued Photometric data

no #	ref	X [px]	Y [px]	V [mag]	(B – V) [mag]	M_V [mag]	(B – V) ₀ [mag]
176	T 58	312.02	1289.90	12.425	0.339	0.525	0.009
177	EV 121	578.36	1291.90	15.956	1.126	4.056	0.796
178	-	213.07	1291.97	16.642	1.322	4.742	0.992
179	T 83	1845.63	1296.59	9.581	0.020	-2.319	-0.310
180	-	418.82	1306.86	16.830	1.286	4.930	0.956
181	-	316.03	1310.79	17.028	1.935	5.128	1.605
182	EV 104	1303.33	1319.82	15.217	1.000	3.317	0.670
183	-	414.92	1321.43	14.659	0.837	2.759	0.507
184	-	153.17	1340.29	15.929	1.199	4.029	0.869
185	-	1935.35	1355.92	15.803	1.011	3.903	0.681
186	-	1868.70	1357.27	15.862	1.005	3.962	0.675
187	-	992.20	1359.94	16.896	1.131	4.996	0.801
188	-	182.27	1360.00	16.524	1.882	4.624	1.552
189	-	136.86	1361.14	14.973	0.814	3.073	0.484
190	EV 103	1308.64	1367.22	16.275	1.087	4.375	0.757
191	-	1678.35	1369.76	15.107	0.876	3.207	0.546
192	-	986.65	1388.20	15.407	1.158	3.507	0.828
193	-	1634.02	1391.19	15.577	0.950	3.677	0.620
194	T 4	2011.94	1391.19	13.425	1.053	1.525	0.723
195	T 82	1707.91	1404.01	13.222	0.963	1.322	0.633
196	EV 102	1360.30	1409.28	14.729	0.802	2.829	0.472
197	EV 514	1548.60	1412.10	14.088	0.633	2.188	0.303
198	T 55	849.95	1418.74	12.827	0.627	0.927	0.297
199	-	1237.07	1419.28	16.019	1.093	4.119	0.763
200	-	1797.97	1435.41	15.211	0.929	3.311	0.599
201	T 56	863.37	1439.33	13.828	0.893	1.928	0.563
202	-	492.36	1443.38	16.411	1.590	4.511	1.260
203	T 57	418.35	1454.55	10.690	0.190	-1.210	-0.140
204	EV 127	904.69	1458.22	14.628	0.915	2.728	0.585
205	-	42.27	1462.05	14.396	2.072	2.496	1.742
206	-	663.53	1463.84	15.912	0.966	4.012	0.636
207	-	1765.15	1465.00	16.533	1.117	4.633	0.787
208	-	84.05	1474.30	16.125	1.286	4.225	0.956
209	-	223.36	1476.16	16.487	1.421	4.587	1.091
210	-	1455.78	1489.89	16.119	1.355	4.219	1.025
211	EV 126	794.32	1490.92	15.320	0.881	3.420	0.551
212	T 81	1630.73	1491.70	12.691	1.900	0.791	1.570
213	EV 128	1552.35	1516.75	15.825	1.331	3.925	1.001
214	-	1679.66	1526.65	15.995	0.996	4.095	0.666
215	-	906.80	1527.87	16.612	1.157	4.712	0.827
216	-	1479.14	1528.07	16.472	1.038	4.572	0.708
217	-	374.19	1529.61	16.395	1.522	4.495	1.192
218	-	495.27	1543.18	16.943	1.102	5.043	0.772
219	-	156.18	1550.33	14.952	1.051	3.052	0.721
220	-	1047.89	1558.93	16.671	2.027	4.771	1.697
221	-	154.93	1558.95	16.539	1.190	4.639	0.860
222	-	811.08	1559.72	16.820	1.531	4.920	1.201
223	-	48.92	1570.62	15.104	1.995	3.204	1.665
224	-	1102.75	1582.05	16.358	1.123	4.458	0.793
225	-	1865.21	1586.25	15.578	0.886	3.678	0.556
226	T 80	1494.10	1600.21	13.342	0.780	1.442	0.450
227	-	1853.22	1609.97	16.519	0.584	4.619	0.254
228	-	540.81	1629.21	15.321	0.923	3.421	0.593
229	-	1003.84	1630.04	16.503	1.555	4.603	1.225
230	-	485.73	1643.99	15.383	1.320	3.483	0.990
231	-	1356.33	1681.92	16.414	1.181	4.514	0.851
232	-	1167.04	1682.17	16.032	0.995	4.132	0.665
233	-	1149.45	1684.80	15.258	0.929	3.358	0.599

cross references according to: T ... Thé (1965), EV ... Evans (1978),
F ... Fitzgerald et al. (1978)

Table A1 – *continued* Photometric data

no #	ref	X [px]	Y [px]	V [mag]	(B – V) [mag]	M_V [mag]	(B – V) ₀ [mag]
234	-	1855.72	1696.06	16.588	1.236	4.688	0.906
235	T 79	1558.33	1700.24	13.480	0.783	1.580	0.453
236	-	1437.65	1701.57	14.253	0.779	2.353	0.449
237	-	248.32	1702.52	17.885	1.871	5.985	1.541
238	T 62	82.90	1703.12	12.942	0.828	1.042	0.498
239	T 77	1876.77	1711.86	12.507	0.916	0.607	0.586
240	-	1652.13	1714.77	16.039	1.002	4.139	0.672
241	-	368.10	1720.81	15.411	1.304	3.511	0.974
242	EV 125	787.44	1721.21	15.718	1.054	3.818	0.724
243	EV 140	755.81	1732.73	14.914	1.529	3.014	1.199
244	-	345.34	1734.22	14.181	2.003	2.281	1.673
245	-	365.95	1750.00	15.843	1.045	3.943	0.715
246	-	319.94	1752.38	16.910	2.713	5.010	2.383
247	-	901.91	1752.96	16.854	1.268	4.954	0.938
248	-	1639.58	1772.67	16.486	1.071	4.586	0.741
249	EV 122	558.13	1775.02	14.052	0.754	2.152	0.424
250	-	1255.14	1777.12	15.439	1.443	3.539	1.113
251	-	1080.34	1784.27	15.613	0.895	3.713	0.565
252	EV 123	665.71	1792.36	14.396	1.174	2.496	0.844
253	EV 124	711.27	1793.36	15.343	1.170	3.443	0.840
254	-	72.90	1797.44	15.741	1.221	3.841	0.891
255	-	409.24	1799.02	16.521	1.188	4.621	0.858
256	-	1186.89	1799.37	15.286	0.919	3.386	0.589
257	T 71	1253.82	1808.40	12.794	0.867	0.894	0.537
258	-	2016.97	1814.63	14.563	1.018	2.663	0.688
259	-	125.07	1833.07	16.374	1.533	4.474	1.203
260	-	846.68	1838.83	16.057	1.238	4.157	0.908
261	T 78	1713.86	1844.37	12.375	0.779	0.475	0.449
262	T 63	193.20	1848.21	12.487	0.671	0.587	0.341
263	-	915.88	1852.10	17.024	2.334	5.124	2.004
264	-	106.20	1859.70	15.449	0.997	3.549	0.667
265	-	1820.86	1863.28	15.305	1.167	3.405	0.837
266	T 64	290.91	1864.59	11.234	0.769	-0.666	0.439
267	T 10	574.28	1865.66	10.048	-0.016	-1.852	-0.346
268	-	1769.05	1868.72	15.043	1.169	3.143	0.839
269	-	1606.88	1870.61	16.628	1.209	4.728	0.879
270	EV 133	1302.32	1875.69	16.390	2.501	4.490	2.171
271	-	783.40	1880.84	13.844	1.246	1.944	0.916
272	-	1376.96	1894.95	15.457	2.191	3.557	1.861
273	T 70	985.36	1912.30	13.074	0.502	1.174	0.172
274	-	2016.04	1921.81	14.643	0.912	2.743	0.582
275	T 65	443.72	1927.54	10.629	1.296	-1.271	0.966
276	-	1021.39	1928.14	15.421	0.823	3.521	0.493
277	-	807.00	1932.98	15.108	1.265	3.208	0.935
278	-	995.31	1948.07	16.408	2.347	4.508	2.017
279	-	1194.13	1957.44	15.576	1.264	3.676	0.934
280	-	1201.84	1975.30	14.674	0.858	2.774	0.528
281	T 69	876.93	1980.01	12.777	0.896	0.877	0.566
282	-	1948.21	1983.77	15.008	0.865	3.108	0.535
283	-	176.35	1987.67	15.584	1.110	3.684	0.780
284	-	716.69	1991.23	14.702	2.120	2.802	1.790
285	EV 316	1754.04	1992.89	14.539	0.739	2.639	0.409
286	-	35.14	2016.29	16.176	1.735	4.276	1.405
287	-	1224.00	2018.87	15.302	1.108	3.402	0.778
288	-	1162.16	2022.13	14.807	0.997	2.907	0.667
289	-	424.21	2022.17	16.411	1.878	4.511	1.548

cross references according to: T ... Thé (1965), EV ... Evans (1978),
F ... Fitzgerald et al. (1978)